Computers and Chemical Engineering 91 (2016) 343–351

Contents lists available at ScienceDirect

Computers and Chemical Engineering

journal homepage: www.elsevier.com/locate/compchemeng

Time-optimal control of diafiltration processes in the presence of membrane fouling

Martin Jelemenský[a,*], Ayush Sharma[a], Radoslav Paulen[a,b], Miroslav Fikar[a]

[a] Faculty of Chemical and Food Technology, Slovak University of Technology in Bratislava, Radlinskeho 9, Bratislava, Slovakia
[b] Department of Chemical and Biochemical Engineering, Technische Universität Dortmund, Emil-Figge-Strasse 70, 44221 Dortmund, Germany

ARTICLE INFO

Article history:
Received 24 September 2015
Received in revised form 8 April 2016
Accepted 11 April 2016
Available online 27 April 2016

Keywords:
Optimal control
Membrane fouling
Pontryagin's minimum principle
Diafiltration

ABSTRACT

This paper deals with time-optimal operation of batch diafiltration processes in the presence of membrane fouling. Fouling causes a decrease in the effective membrane area and, hence, an increase in processing time. In this work we study a time-optimal operation with several fouling models available in literature. Pontryagin's minimum principle is applied to characterize the structure of the optimal operation which voids any further on-line optimization. Due to the specific structure of the problem, it is possible, in several problem setups, to derive and verify an explicit analytic solution. Obtained results are applied in case studies where we provide a comparison between traditional operation and the proposed time-optimal operation. In cases, where the optimal operation cannot be identified analytically, we analyze the performance of sub-optimal control derived from neighboring analytical solution and compare it to optimal operation found via numerical optimization techniques.

1. Introduction

Diafiltration (DF) membrane processes separate solutes in a solution based on differences in molecular size. Membranes retain high molecular weight components and let low molecular weight components pass through. These processes have found a wide range of applications. In food industry they are used for fruit juice clarification (Yazdanshenas et al., 2005). In pharmaceutical industry the membrane separation is used for different aims like albumin production from human blood (Aspelund and Glatz, 2010) and anti body preparation (Luo et al., 2004). Biotechnological industries use membrane processes for enzyme concentration and the removal of impurities like peptides and salts (Li et al., 2006).

One of main issues in membrane separation is membrane fouling. It causes a decrease in effective membrane area due to the deposit of the solutes in or on the membrane pores. This results in an increase of the processing time to reach the desired purification goal. Moreover, the fouled membrane needs to be cleaned or replaced (Luján-Facundo et al., 2015) which further increases the operational costs. For these reasons modeling of the fouling behavior has gained importance. The pioneering work of Hermia (1982) presented a unified fouling model describing this behavior from which four standard fouling models can be derived. These express the decrease in effective membrane area (Bolton et al., 2006) or the permeate flux (Vela et al., 2008). These models have, however, an empirical character so they have to be tailored to the application at hand by conducting experiments and by subsequent model discrimination and identification of the model parameters. In Charfi et al. (2012) the authors showed that numerical optimization techniques can be employed to predict types of the fouling mechanism using experimental data. Advanced method based on on-line estimation of the fouling using Kalman filter was discussed in Jelemenský et al. (2016).

In this paper we consider a batch diafiltration process, which operates under constant pressure and temperature. Diafiltration processes use a solute-free solvent (diluant e.g. water) to control the process via influencing the concentrations of solutes. Ng et al. (1976) derived conditions of optimal switching concentration for a standard, yet simple, DF process. Foley (1999) proposed to optimize switching times in the arbitrarily chosen sequence of the traditional control modes such as concentration mode or constant-volume diafiltration. Therein it was also shown that different control strategies of diluant addition can result in time-optimal operation or minimal diluant consumption. Procedures based on numerical optimization have been investigated in Takači et al. (2009) and Fikar et al. (2010), where numerical methods like control vector parametrization and orthogonal collocation were used to compute the optimal solution through approximation of control and state trajectories. These methods can be applied for arbitrary optimal

* Corresponding author.
E-mail address: martin.jelemensky@stuba.sk (M. Jelemenský).

http://dx.doi.org/10.1016/j.compchemeng.2016.04.018
0098-1354/

List of symbols

A	membrane area (m^2)
c_1	concentration of macro-solute – product (mol/m^3)
c_2	concentration of the first micro-solute – impurity (mol/m^3)
H	Hamiltonian function
J	permeate flux (m/h)
J_0	permeate flux of unfouled membrane (m/s)
k	mass transfer coefficient (m/h)
K_g	cake-layer formation constant (s/m^2)
K_i	intermediate fouling constant (1/m)
K_s	standard (internal) fouling constant ($1/m^{1/2}/s^{1/2}$)
K_c	complete fouling constant (1/s)
q	permeate flow (m^3/h)
t	operation time (h)
t_f	processing time (h)
V	volume in feed tank (m^3)
R	rejection coefficient
S	singular surface

Greek symbols

α	proportionality factor of diluant flow to permeate flow
λ_i	ith adjoint variable

Subscripts

0	initial
f	final

Abbreviations

C	concentration (mode)
CVD	constant-volume diafiltration
D	dilution (mode)

control problem. Another way to solve it is to employ analytical methods. The advantage of analytical methods compared to numerical is the exact solution without any approximation. A fully analytical solution for optimal membrane operation without fouling was derived in Paulen et al. (2012) for arbitrarily initial and final conditions (e.g. concentrations). In Jelemenský et al. (2014) preliminary results on time-optimal operation in the presence of membrane fouling have been published. A combination of numerical and analytical methods was used to compute the optimal control profiles.

In this paper we extend the work published in Jelemenský et al. (2015) and we investigate the time-optimal operation of a diafiltration process in the presence of membrane fouling. Pontryagin's minimum principle is applied to derive the analytical optimal operation in the presence of membrane fouling and to deduce the structure of the optimal solution. We assume an explicit dependency of permeate flux on processing time as proposed by Vela et al. (2008).

The main novelty of this paper is the complete characterization of the time-optimal operation of a diafiltration process in the presence of membrane fouling. There are no restrictions to the specific form of a fouling model or mechanism. We only assume the functional dependency of fouling on the operation time. The resulting optimal operation derived in this paper is given by simple rules and avoids any on-line optimization. We also show that if the optimal operation cannot be obtained analytically a neighboring analytical solution, with sub-optimal performance, gives similar results to the time-optimal operation.

The paper is organized as follows. In the next section, the process description and model are presented. In Section 3 detailed analysis of membrane fouling and modeling of fouling behavior is described. Section 4.1 defines the overall optimization problem. Section 4.2 gives the main theoretical contributions of the paper. Optimal operation of diafiltration processes in the presence of membrane fouling is derived. Finally, simulation studies are provided in Section 5 to discuss and analyze the proposed solution.

2. Process description and modeling

We study a generalized batch diafiltration process shown in Fig. 1. The process operates under constant pressure and temperature. The batch diafiltration process consists of a feed tank and a membrane. The process solution containing a solvent and two solutes (macro- and micro-solute) is brought from the feed tank to the membrane. The stream which is rejected by the membrane (retentate) is taken back into the feed tank. The permeate stream leaves the system at a given flow-rate $q = AJ$, where A represents the membrane area and J is the permeate flux subjected to unit membrane area. The permeate stream is often a function of both concentrations. In addition, it is also a function of time as it decreases when fouling occurs.

Process control is achieved by adjusting the flow-rate of the solute-free solvent (diluant) into the feed tank. The control variable is denoted by α and it is defined as a ratio between the inflow of the diluant and the permeate flow-rate q. There are several commonly used control modes such as concentration mode (C) with $\alpha = 0$, constant-volume diafiltration (CVD) with $\alpha = 1$, and dilution (D) where $\alpha = \infty$. The dilution mode is characterized by a certain amount of diluant added instantaneously into the feed tank. Traditional operation strategies used in the industry then consist of sequences of the individual control modes (e.g. C-CVD).

Mass balances can be used to obtain the process model. The balance of each solute can be written as (Kovács et al., 2009)

$$\frac{dc_i}{dt} = \frac{c_i q}{V}(R_i - \alpha), \quad c_i(0) = c_{i,0}, \quad i = 1, 2, \ldots \tag{1}$$

where V is the feed tank volume at time t and $i = 1, 2$ denotes the macro-solute and micro-solute, respectively. R_i is the so-called observed (measured) rejection coefficient. The rejection coefficient is a dimensionless number between 0 and 1 that measures the ability of the membrane to retain the ith species. It is defined as

$$R_i = 1 - \frac{c_{p,i}}{c_i}, \tag{2}$$

where $c_{p,i}$ stands for the concentration of the ith species in the permeate.

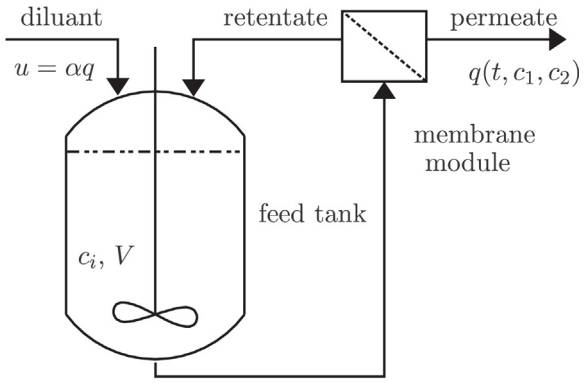

Fig. 1. Schematic representation of a generalized diafiltration process.

The total mass balance can be written as

$$\frac{dV}{dt} = u - q = (\alpha - 1)AJ, \quad V(0) = V_0, \tag{3}$$

with V_0 being the initial volume of the processed solution.

2.1. Modeling with perfect macro-solute rejection

Rejection coefficients R_i can be functions of both concentrations. The special, yet industrially relevant, case assumes that $R_1 = 1$ and $R_2 = R_2(c_1, c_2)$. This means that the membrane is absolutely impermeable for the macro-solute and permeability of micro-solute is a function of both concentrations. Therefore, the macro-solute will be completely rejected by the membrane and concentrated in the feed tank.

As the rejection of the macro-solute is perfect, its total mass in the system is constant. Thus, $c_1(t)V(t) = c_{1,0}V_0$ and the differential equation (3) can be omitted. The model is then of the form

$$\frac{dc_1}{dt} = c_1^2 \frac{AJ}{c_{1,0}V_0}(1 - \alpha), \quad c_1(0) = c_{1,0}, \tag{4}$$

$$\frac{dc_2}{dt} = c_1 c_2 \frac{AJ}{c_{1,0}V_0}(R_2 - \alpha), \quad c_2(0) = c_{2,0}. \tag{5}$$

3. Membrane fouling

Membrane fouling belongs to one of the main obstacles in the membrane separation processes. The main cause of the membrane fouling is the deposit of the solutes in/on the membrane pores. As a consequence, a decrease of the effective membrane area occurs. The membrane fouling depends on several factors. It is more pronounced when strong concentration (gel) polarization effects occur. During filtration, retained macro-solutes form a so-called gel layer over the surface of the membrane (Baker, 2012). This increases the likeliness of the macro-solute particles to interact with the surface of the membrane and to block its pores. The precise mechanisms of such interaction are introduced below. Additionally the factors that influence the membrane fouling, both quantitatively and qualitatively, are represented by feed properties, membrane material, temperature, and pressure (Zhao et al., 2000).

Hence, the inevitable phenomenon of membrane fouling results in the decrease of permeate flow. As the consequence of the decrease of the permeate flow the overall processing time increases. Moreover, once the membrane becomes significantly fouled cleaning has to be performed. Also if the cleaning is insufficient the membrane has to be replaced. All this leads to an increase of operational costs.

Modeling of fouling became highly important in the past years. In Hermia (1982) a unified fouling model for dead-end filtration systems was derived in terms of total permeate flux and time and reads as

$$\frac{d^2t}{dV_p^2} = K\left(\frac{dt}{dV_p}\right)^n, \tag{6}$$

where V_p represents the permeate volume, t is time, and K is the fouling rate constant. Four classical fouling models are characterized by different values of n. We recognize cake filtration ($n = 0$), intermediate blocking ($n = 1$), standard (internal) blocking ($n = 3/2$), and complete pore blocking ($n = 2$) models. The corresponding differential equation for permeate flux can then be derived as (Bolton et al., 2006; Vela et al., 2008)

$$\frac{dJ}{dt} = -KA^{2-n}J^{3-n}. \tag{7}$$

If n, K, A are considered constant, this differential equation can be solved to give an explicit solution $J(t, n, K, A, J_0)$ where J_0 represents initial flux at time $t = 0$. It can happen that the fouling parameters are not constant or that different fouling phenomena occurs in parallel or in series. For this reason, it is crucial to determine on-line or off-line both the fouling rate and the fouling model. In our recent study (Sharma et al., 2016) we assumed constant area and estimated the fouling model and the fouling rate constants. Another approach was studied in Jelemenský et al. (2014), where the fouling considered effective membrane area decrease in time due to deposit of the solutes.

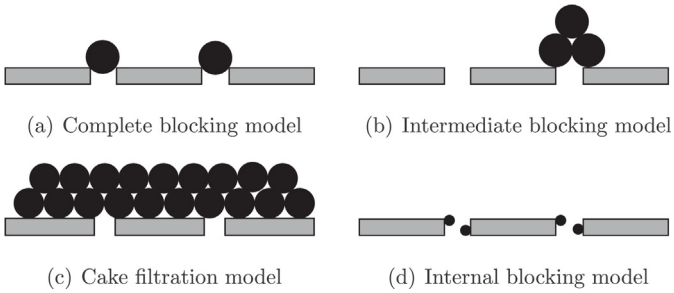

Fig. 2. Graphical representation of the four classical fouling models developed by Hermia.

To apply this model to cross-flow systems considered in this study, we propose to substitute the initial flux $J_0(t = 0)$ by the unfouled flux $J_0(c_1, c_2)$ that depends on actual concentrations. This will make it possible to unify procedures and results for systems with and without fouling.

Fig. 2 shows graphical representation of the individual fouling mechanisms, i.e. complete blocking model (Fig. 2(a)), intermediate blocking model (Fig. 2(b)), cake filtration model (Fig. 2(c)) and the internal blocking model (Fig. 2(d)). These models differ in the way the molecules deposit in/on the membrane.

3.1. Complete pore blocking model

Complete pore blocking model considers that solutes which are brought to the membrane surface will seal the membrane pores (Fig. 2(a)). Flow through such pores is no longer possible. The molecules which deposit on the membrane surface are larger than the membrane pores. The model can be derived from (6) after setting the parameter $n = 2$. The model is expressed in terms of permeate flux versus time and is of the form

$$\ln J = \ln J_0 - K_c t, \tag{8}$$

where J is the permeate flux subject to unit area in m/s, J_0 is the permeate flux of unfouled membrane and $K_c = K$ represents the fouling rate constant in 1/s. We can notice that the fouling rate does not depend on the membrane area.

3.2. Intermediate blocking model

The intermediate pore blocking model again assumes that all solutes brought to the membrane surface will block the membrane pores. However, in this case the solutes can deposit on each others as illustrated in Fig. 2(d). The parameter n is equal to 1 and the permeate flux is of the form

$$\frac{1}{J} = \frac{1}{J_0} + K_i t, \tag{9}$$

with $K_i = KA$ being the fouling rate constant in 1/m. In this case the fouling rate constant is a linear function of the membrane area.

3.3. Cake filtration model

The fouling according to this model is caused by deposition of solutes on the surface of the membrane. The process repeats itself, that is with each cycle the solutes keep depositing over the previously deposited solutes and this results in formation of a multi-layered cake of solutes, as it is shown in Fig. 2(c). The parameter n in this case is equal to 0 and the permeate flux is of the form

$$\frac{1}{J^2} = \frac{1}{J_0^2} + K_g t, \tag{10}$$

where $K_g = 2KA^2$ is the fouling constant with the unit s/m^2.

3.4. Internal blocking model

On the contrary to previous fouling models discussed, this model defines fouling internally. The model describes that the solutes instead of depositing on the surface of the membrane, are small enough to clog the pores of the membrane. The phenomenon results in the reduction of pore diameter and hence in a decrease of the permeate flux. The parameter n is equal to 3/2 and the flux is of the form

$$\frac{1}{\sqrt{J}} = \frac{1}{\sqrt{J_0}} + K_s t \tag{11}$$

where $K_s = \frac{1}{2}KA^{1/2}$ is the fouling rate constant in 1/m$^{1/2}$/s$^{1/2}$.

4. Optimal operation

4.1. Problem definition

The optimization goal is to find such time-dependent function $\alpha(t)$ which guarantees the transition from given initial to final concentrations in minimum time. We assume that the membrane is absolutely impermeable to macro-solute ($R_1 = 1$), the permeability of micro-solute changes as a function of concentrations, and is expressed using rejection coefficient $R_2 = R_2(c_1, c_2)$. Finally, we assume that the unfouled flux is a known function of both concentrations $J_0(c_1, c_2)$ and the fouling model of the flux J is given. The optimization problem then reads as:

$$\mathcal{J}^* = \min_{\alpha(t)} \int_0^{t_f} 1\,\mathrm{d}t, \tag{12a}$$

s.t.

$$\dot{c}_1 = c_1^2 \frac{AJ}{c_{1,0}V_0}(1-\alpha), \quad c_1(0) = c_{1,0}, \tag{12b}$$

$$\dot{c}_2 = c_1 c_2 \frac{AJ}{c_{1,0}V_0}(R_2-\alpha), \quad c_2(0) = c_{2,0}, \tag{12c}$$

$$c_1(t_f) = c_{1,f}, \tag{12d}$$

$$c_2(t_f) = c_{2,f}, \tag{12e}$$

$$J = J(t, J_0(c_1, c_2), K, n), \tag{12f}$$

$$\alpha \in [0, \infty). \tag{12g}$$

We note that the optimization problem for a generalized diafiltration setup ($R_1 = R_1(c_1, c_2)$) possesses a similar structure where the Eqs. (12b) and (12c) are replaced with Eqs. (1) for $i = 1, 2$ and (3).

4.2. Characterization of the optimal operation

We use Pontryagin's minimum principle (PMP) (Pontryagin et al., 1962; Bryson and Ho, 1975; Srinivasan et al., 2003) to identify the candidates for optimal control described by Eq. (12). A care has to be taken as the process model depends explicitly on time, thus the problem is non-autonomous.

There are two possible approaches to handle optimal control of non-autonomous systems. The first approach considers time explicitly in the process model. Then, the optimal Hamiltonian function is zero only at final time. Therefore, there are two variables (concentrations) and PMP has to supply two equations for optimality. The second approach adds an additional state variable $\dot{x}_a = 1$ with initial condition $x_a(0) = 0$ and replaces t with x_a. Therefore, the new problem is autonomous with increased number of variables. In this case, Hamiltonian function is zero along the optimal trajectory and this fact can be used to provide additional conditions for finding an optimal solution.

Our derivation will use the first approach. Let us define the state vector $\boldsymbol{x} = (c_1, c_2)^T$ and rewrite the process differential equations as affine functions of control α

$$\dot{\boldsymbol{x}} = \boldsymbol{f}(t, \boldsymbol{x}) + \boldsymbol{g}(t, \boldsymbol{x})\alpha, \tag{13}$$

The Hamiltonian function can then be constructed as

$$H(t, \boldsymbol{x}, \boldsymbol{\lambda}, \alpha) = 1 + \boldsymbol{f}^T(t, \boldsymbol{x})\boldsymbol{\lambda} + \boldsymbol{g}^T(t, \boldsymbol{x})\boldsymbol{\lambda}\alpha = H_0(t, \boldsymbol{x}, \boldsymbol{\lambda}) + H_\alpha(t, \boldsymbol{x}, \boldsymbol{\lambda})\alpha, \tag{14}$$

where $\boldsymbol{\lambda} = (\lambda_1, \lambda_2)^T$ is the vector of adjoint variables defined from

$$\dot{\boldsymbol{\lambda}} = -\frac{\partial H}{\partial \boldsymbol{x}} = -(\boldsymbol{f}_x + \boldsymbol{g}_x\alpha)\boldsymbol{\lambda}, \tag{15}$$

where

$$\boldsymbol{f}_x(t, \boldsymbol{x}) = \frac{\partial \boldsymbol{f}^T(t, \boldsymbol{x})}{\partial \boldsymbol{x}}, \quad \boldsymbol{g}_x(t, \boldsymbol{x}) = \frac{\partial \boldsymbol{g}^T(t, \boldsymbol{x})}{\partial \boldsymbol{x}}. \tag{16}$$

Since the Hamiltonian is affine in α, its minimum is attained with α on its boundaries as follows

$$\alpha = \begin{cases} 0 & \text{if } H_\alpha > 0, \\ \infty & \text{if } H_\alpha < 0. \end{cases} \tag{17}$$

If the Hamiltonian is singular in α, the singular case is characterized by equations $H_\alpha = 0$, $\dot{H}_\alpha = 0$. This gives a set of equations which are linear in adjoint variables

$$H_\alpha(t, \boldsymbol{x}, \boldsymbol{\lambda}) = \boldsymbol{g}^T\boldsymbol{\lambda} = 0, \tag{18}$$

$$\dot{H}_\alpha(t, \boldsymbol{x}, \boldsymbol{\lambda}) = \boldsymbol{h}^T\boldsymbol{\lambda} = \left(\boldsymbol{g}_x\boldsymbol{f} - \boldsymbol{f}_x\boldsymbol{g} + \frac{\partial H_\alpha}{\partial t}\right)^T \boldsymbol{\lambda} = 0. \tag{19}$$

Elimination of $\boldsymbol{\lambda}$ from (18) and (19) results in characterization of the singular surface:

$$S(t, c_1, c_2) = (R_2 - 1)\left(J + c_1\frac{\partial J}{\partial c_1} + c_2\frac{\partial J}{\partial c_2}\right) + J\left(c_1\frac{\partial R_2}{\partial c_1} + c_2\frac{\partial R_2}{\partial c_2}\right) = 0. \tag{20}$$

Note that the expression (20) is formally identical to the one without fouling, as derived in Paulen et al. (2012). The only difference lies in the fact that J (and thus S) is not only a function of concentrations but also of time. For example, an expression for the singular surface in case of $R_2 = 0$ and the intermediate blocking model boils down to

$$S(t, c_1, c_2) = J_0 + c_1\frac{\partial J_0}{\partial c_1} + c_2\frac{\partial J_0}{\partial c_2} + K_i J_0^2 t = 0. \tag{21}$$

The above relation clearly shows the shift in the optimal operation with fouling ($K_i \neq 0$) and without fouling ($K_i = 0$).

To obtain the control which keeps the states on the singular surface, we differentiate the singular surface described by Eq. (20)

w.r.t. time. The obtained singular control is:

$$\alpha(t, c_1, c_2) = \frac{(\partial S)/(\partial c_1)c_1 + (\partial S)/(\partial c_2)c_2 R_2}{(\partial S)/(\partial c_1)c_1 + (\partial S)/(\partial c_2)c_2} + \frac{(\partial S)/(\partial t)}{(c_1 JA)/(c_{1,0}V_0)((\partial S)/(\partial c_1)c_1 + (\partial S)/(\partial c_2)c_2)}. \quad (22)$$

This can be again formally separated into two parts: the first one corresponding to the unfouled singular control and the second one handling the influence of fouling on the optimal operation.

Following the analysis of the unfouled case derived in Paulen et al. (2012), the optimal operation consists of the following three steps:

1. In the first step we use either concentration mode or pure dilution mode (see Eq. (17)) until the condition $S(t, c_1, c_2) = 0$ is met. The choice of the appropriate mode depends on initial conditions.
2. During the second step we stay on singular surface where the singular control (Eq. (22)) is used.
3. The last step is again the operation with either concentration mode or pure dilution until the final conditions for concentrations are met.

Note that any step can be missing from the optimal operation. This depends solely on the initial and final conditions. For instance, if there does not exist any three-step strategy fulfilling the final conditions, the middle step is skipped, and the optimal control is saturated on constraints.

5. Case studies

We consider three case studies where the fouling is described by intermediate pore blocking model (Eq. (9)). We apply the proposed time-optimal control strategy to the case studies and compare it with the traditional control strategy (C-CVD).

5.1. Case study 1

In this case study we use a classical setup of the separation of two solutes by diafiltration with constant rejection coefficients. The permeate flux is the simplest possible derivate of mass-transfer theory (Fick's law) and is of the form

$$J_0(c_1) = k \ln \frac{c_{\text{lim}}}{c_1}, \quad (23)$$

where c_{lim} is the limiting concentration of the product and k is the mass transfer coefficient. We also consider that the rejection coefficients are constant ($R_1 = 1$ and $R_2 = 0$). This means that the membrane is absolutely impermeable for macro-solute (c_1) and that the micro-solute (c_2) can pass freely through the membrane pores.

The goal is to drive the concentrations from the initial point $[c_{1,0}, c_{2,0}] = [3.3\ \text{g/dL}, 5.5\ \text{g/dL}]$ to the final point $[c_{1,\text{f}}, c_{2,\text{f}}] = [9.04\ \text{g/dL}, 0.64\ \text{g/dL}]$ for 100 dL of solution and for the employed membrane area of 1 m^2. The limiting concentration of the product is 56 g/dL and the mass transfer coefficient is $k = 12.439$ m/h. The singular surface can be derived from Eq. (20) and is of the form

$$S(t, c_1) = \left(\ln \frac{c_{\text{lim}}}{c_1} - 1\right) + 2tkK_i \ln \frac{c_{\text{lim}}}{c_1} = 0. \quad (24)$$

If we differentiate the singular surface with respect to time we obtain the singular surface

$$\alpha(t, c_1) = 1 + \frac{K_i c_{1,0} V_0 (K_i J_0 t + 1)\left[\ln((c_{\text{lim}})/(c_1))(K_i J_0 t + 1) - 2\right]}{A c_1 (K_i t(2k + J_0) + 1)}, \quad (25)$$

where V_0 stands for the initial volume. We can observe that, besides concentrations, singular surface and control also depend on fouling rate and time. Note that when no fouling is present, the optimal operation boils down to the classical result, i.e. the CVD step should be commenced when $c_1 = c_{\text{lim}}/e$.

Using the presented theoretical results and knowledge on initial and final conditions, the time-optimal operation in the presence of fouling comprises a sequence of following three steps:

1. The first step is the concentration mode $\alpha = 0$ till the singular surface (Eq. (24)) is reached.
2. Then, in the second step, the states reside on the singular surface with the singular control (Eq. (25)). This step is performed until the condition $c_1(t)/c_2(t) = c_{1,\text{f}}/c_{2,\text{f}}$ is satisfied.
3. In the last step we perform pure dilution mode with $\alpha = \infty$ to reach the final concentrations.

Fig. 3 depicts the optimal control strategy (states and control) for the minimum-time operation for different fouling rates. The control structure in all the cases is the three-step strategy described above. The circle in the state diagram represents the initial concentrations and the cross depicts the final ones. We can observe

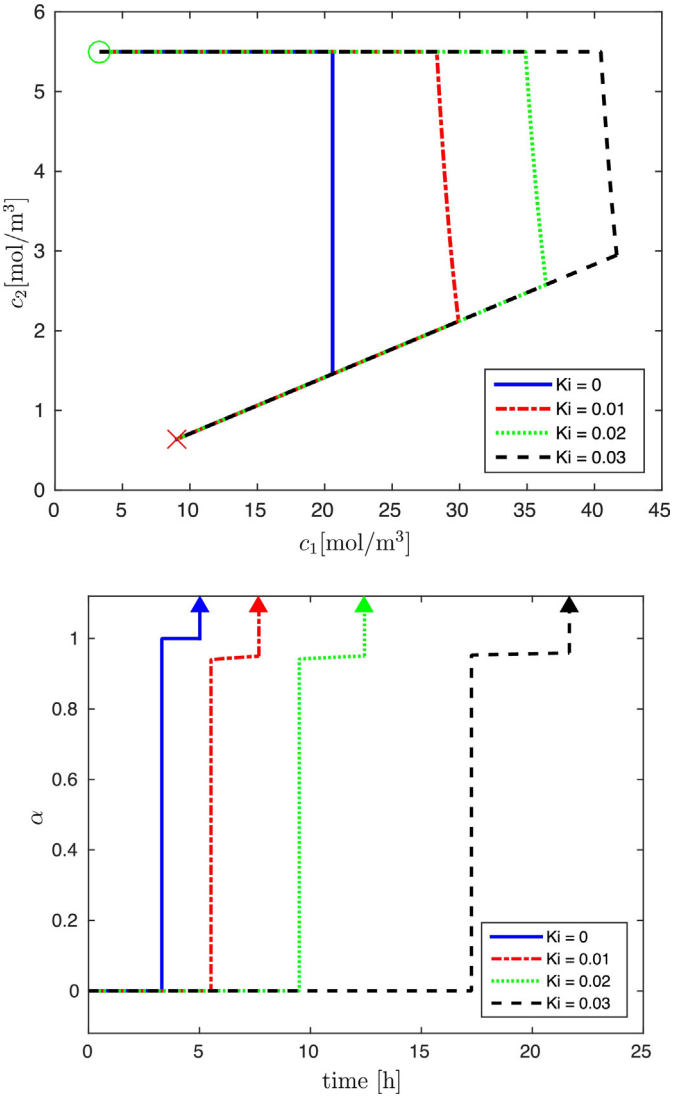

Fig. 3. Comparison of different control strategies (top – state space, bottom – control profiles).

Table 1
Time-optimal operation compared to traditional operation for different fouling rates.

K_i (10^{-3} m^{-1})	Minimum time t_f (h)	Switching time t_s (h)	C-CVD t_f (h)	Δ (%)
0	5.01	3.31	5.61	11.97
10	7.68	5.52	11.70	52.34
20	12.44	9.49	28.37	128.05
30	21.67	17.26	78.02	260.04

Table 2
Time-optimal operation compared to traditional operation for different fouling rates.

K_i (10^{-3} m^{-1})	Minimum time t_f (h)	Switching time t_s (h)	C-CVD t_f (h)	Δ (%)
0	4.49	2.45	4.74	5.57
10	7.24	4.85	10.52	45.30
20	12.02	8.85	26.70	122.13
30	21.27	16.54	75.57	255.29

that the switching concentration to singular surface described by Eq. (24) changes with different fouling rates K_i. Furthermore we can observe that the increase of these values translates to longer processing time, as expected.

Table 1 presents a comparison of the final processing times in case of the proposed minimum-time operation and the traditionally used operation (C-CVD). Moreover, we also report the corresponding switching time (t_s) when the time-optimal operation switches from concentration mode to singular mode. The traditional mode of operation consists of two steps. It starts with the same concentration mode as the proposed approach. However, its second step is constant volume diafiltration ($\alpha = 1$) and it is switched on at $c_1 = c_{1,f}$. Clearly, as fouling pronounces, this diafiltration step is suboptimal causing overall increase of processing time. Further, we can also observe that by the increase of the fouling rate the switching times increase. This is mainly caused by the decrease in the permeate flow and slower reduction of the feed volume, which eventually results in longer time to reach the optimal switching concentration. For the highest rate of fouling considered here, the savings in terms of processing time are almost threefold.

A care must be taken when applying this optimal operation on a real process. The traditional C-CVD operation and model represented by Eq. (23) operate with concentration $c_1 < 10$ g/dL. The proposed optimal operation uses much higher concentrations of macro-solute up to 40 g/dL. Therefore, a new model has to be estimated that also covers this area. Such high concentration can cause strong polarization effects and necessity to move the operation in lower-concentration region. In that case, the singular surface would not be attained and constraint-based operation would be applied as shown in Jelemenský et al. (2014). Moreover, if the rejection coefficient for macro-solute (with concentration c_1) would be less than one, the switching time t_s would be reached later compared to the case when $R_1 = 1$. This is caused by the outflow of the macro-solute from the system, which results in longer time to reach the desired switching concentration. However, in this case numerical optimization would be needed to compute the optimal switching concentration. This is because the time-optimal operation can be derived analytically only in the case when $R_1 = 1$.

5.2. Case study 2

We study separation of lactose (with concentration c_2) from proteins (with concentration c_1). The separation problem was originally formulated in Rajagopalan and Cheryan (1991) and its optimal unfouled control was derived in Paulen et al. (2012). The experimentally verified model for the permeate flux is given as

$$J_0(c_1, c_2) = b_0 + b_1 \ln c_1 + b_2 \ln c_2 = 63.42 - 12.439 \ln c_1 - 7.836 \ln c_2. \quad (26)$$

The permeate flux model can be alternatively rewritten into the form

$$J_0(c_1, c_2) = -b_1 \left(\ln e^{-(b_0)/(b_1)} - \ln c_1 + \ln c_2^{-(b_2)/(b_1)} \right) = -b_1 \ln \frac{e^{-(b_0)/(b_1)} c_2^{-(b_2)/(b_1)}}{c_1}, \quad (27)$$

which resembles the expression for limiting flux (Eq. (23)). However, compared to the previous case study, in this case the limiting macro-solute concentration depends on the concentration of c_2. We will consider the same initial and final concentrations, the membrane area, rejection coefficients and the initial volume as in the previous case study.

The singular surface is of the following form

$$S(t, c_1, c_2) = b_0 + b_1(\ln c_1 + 1) + b_2(\ln c_2 + 1) + K_i t J_0^2 t = 0, \quad (28)$$

and singular control is as follows

$$\alpha(t, c_1, c_2) = \frac{b_1}{b_1 + b_2} + \frac{K_i c_{1,0} V_0 (K_i J_0 t + 1)(2b_1 + 2b_2 + J_0(K_i J_0 t + 1))}{K_i t A c_1 (b_1 + b_2)(2b_1 + 2b_2 - J_0 - 1)}. \quad (29)$$

Here we can easily distinguish the contribution of the fouling to the optimal operation of unfouled membrane system.

The time-optimal operation in the presence of membrane fouling consists of the same three steps as presented in the previous case study. As explained in the previous case study, when different rejection for macro-solute would be considered the switching time would be reached in higher time. In addition, the optimal switching time and the singular control would need to be computed by numerical optimization.

Fig. 4 depicts the optimal control strategy (states and control) for the minimum-time operation for different fouling rates. Compared to the previous case study, the unfouled singular control mode is variable volume diafiltration ($\alpha \approx 0.61$) which changes slightly with increased fouling rate. As in the previous case study, the macro-solute concentration that switches to singular mode increases with the fouling rate and the total processing time increases as well.

Table 2 presents a comparison of the final processing time in case of proposed minimum-time operation and the traditionally used operation (C-CVD). In the table we also show the switching time (t_s) where in the case of time-optimal operation we switch from concentration mode to singular control mode. The differences in the duration of the respective operations get more significant as the fouling rate increases. For the highest rate of fouling considered here, the savings in terms of processing time are almost threefold.

When we compare the two case studies, we can observe different processing times and also different switching times. These differences also result in different savings for the same fouling rates. This is caused mainly due to the fact that in the second case study the limiting concentration for the macro-solute was a function of concentration c_2. We can also observe that this difference in the model of the permeate flux resulted in different expression for singular surface and thus to different singular control.

5.3. Case study 3

The purpose of this study is to show the properties of the proposed approach if some of the assumptions are not satisfied. Namely, we will study a membrane separation process where the rejection of the macro-solute by the membraneis not complete, and

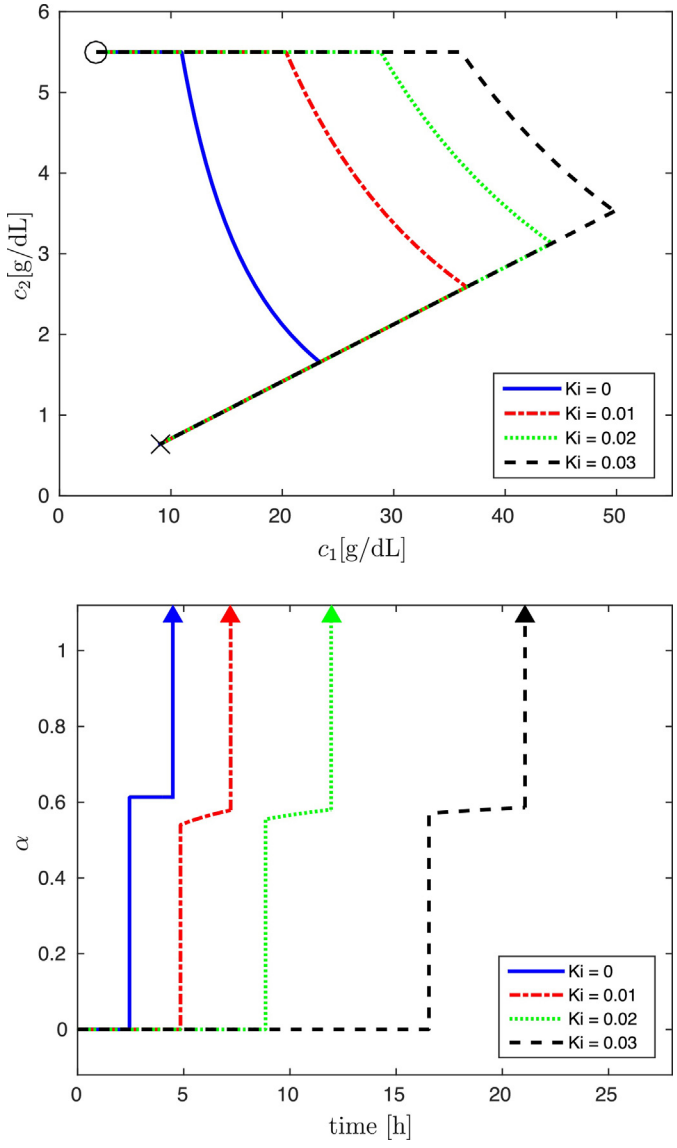

Fig. 4. Comparison of different control strategies (top – state space, bottom – control profiles).

varies according to the concentrations of both solutes. As it was pointed out in Paulen et al. (2015), analytical expressions of singular surface are no longer possible for such a case and the resulting optimal control problem needs to be solved numerically.

The considered process model is taken from Fikar et al. (2010). The original experiment (Kovács et al., 2009) providing the models of permeate flux and rejection coefficients, dealt with separation of technical grade sucrose and sodium chloride in aqueous solvent. Sucrose being the macro-solute (product), and sodium chloride the micro-solute (impurity). The purpose of the experiment was to find the relation between permeate flux, rejection coefficient, and the concentrations. The separation was achieved using cross-flow nanofiltration ($A = 0.45\ \mathrm{m}^2$), as it has the appropriate pore size and structure, applicable for demineralization of saccharides. The experiment was carried out at constant temperature and pressure. The empirical relations for J_0, R_1 and R_2 as functions of component concentrations are as follows:

$$J_0 = S_1(c_2)\,\mathrm{e}^{S_2(c_2)c_1}, \tag{30a}$$

$$R_1 = (z_1 c_2 + z_2)c_1 + (z_3 c_2 + z_4), \tag{30b}$$

Table 3
Experimentally obtained coefficient values for R_1, R_2, and J_0.

i	s_i	w_i	z_i
1	68.1250×10^{-9}	7.8407×10^{-6}	-0.0769×10^{-6}
2	-56.4512×10^{-6}	-4.0507×10^{-3}	-0.0035×10^{-3}
3	32.5553×10^{-3}	1.0585	0.0349×10^{-3}
4	-4.3529×10^{-9}	1.2318×10^{-9}	0.9961
5	3.3216×10^{-6}	-9.7660×10^{-6}	
6	-2.7141×10^{-3}	-1.1677×10^{-3}	

$$R_2 = W_1(c_2)\,\mathrm{e}^{W_2(c_2)c_1}, \tag{30c}$$

where S_1, S_2, W_1, W_2 are

$$S_1 = s_1 c_2^2 + s_2 c_2 + s_3, \tag{31a}$$

$$S_2 = s_4 c_2^2 + s_5 c_2 + s_6, \tag{31b}$$

$$W_1 = w_1 c_2^2 + w_2 c_2 + w_3, \tag{31c}$$

$$W_2 = w_4 c_2^2 + w_5 c_2 + w_6, \tag{31d}$$

and s_{1-6}, z_{1-4} and w_{1-6} are experimentally evaluated coefficients with the process solution (see Table 3).

The intermediate fouling model is considered with values of K_i up to $5\ \mathrm{m}^{-1}$. The maximum value of α is constrained by 1.

Numerical method of orthogonal collocation was used to compute the optimal control and state trajectories. The main idea behind the method is that the state and control trajectories are approximated with piece-wise Lagrange polynomial functions on some chosen number of intervals. The approximation is exact at the collocation points. The roots of Legendre polynomials determine the distribution of these collocation points (Biegler, 1984; Čižniar et al., 2005). In our case we chose 3–7 time intervals, 5 collocation points on states and 3 collocation points on control to find the optimal separation strategy. Differences in final processing times between 3 and 7 time intervals were not significant.

Fig. 5 depicts the optimal trajectory of concentration of sucrose and sodium chloride to drive from initial states (circle) to final states (cross). The figure compares optimal trajectories of sucrose and sodium chloride for both analytical and numerical control approaches with maximum membrane fouling studied ($K_i = 5\ \mathrm{m}^{-1}$). The state trajectory consists of three steps, i.e. concentration mode, diafiltration with time-varying profile of α, and constant volume diafiltration mode. Therefore, the control variable α is equal to 0 in the first step to increase the concentration of both product and impurity. In the second part the control varies in a mid range, and that highly contributes to the concentration increase in our product. The final step is constant volume diafiltration mode with $\alpha = 1$ and directly translates to reduction in impurity to achieve the final product and impurity concentration.

The optimal control trajectory obtained numerically shows some typical oscillations in singular mode due to a low sensitivity of the cost function to this part of the control trajectory. The magnitude and frequency of the oscillations increase as the number of time intervals increase and hence we can see comparatively more oscillations in the seven-step strategy, than three-step or analytical strategy. This is mainly caused due to more optimization variables and numerical insensitivity. In fact, the second step could be replaced, for practical purposes, with a constant α (variable volume diafiltration mode) without a major change in the duration of the operation.

Simulations with other values of the fouling parameter K_i showed the similar behavior, although processing time for lower values of K_i was shorter. Even if the assumptions for the proposed method are not valid, the resulting state and control trajectories are almost optimal and the final processing times are practically the same as those obtained with numerical optimization. This is due

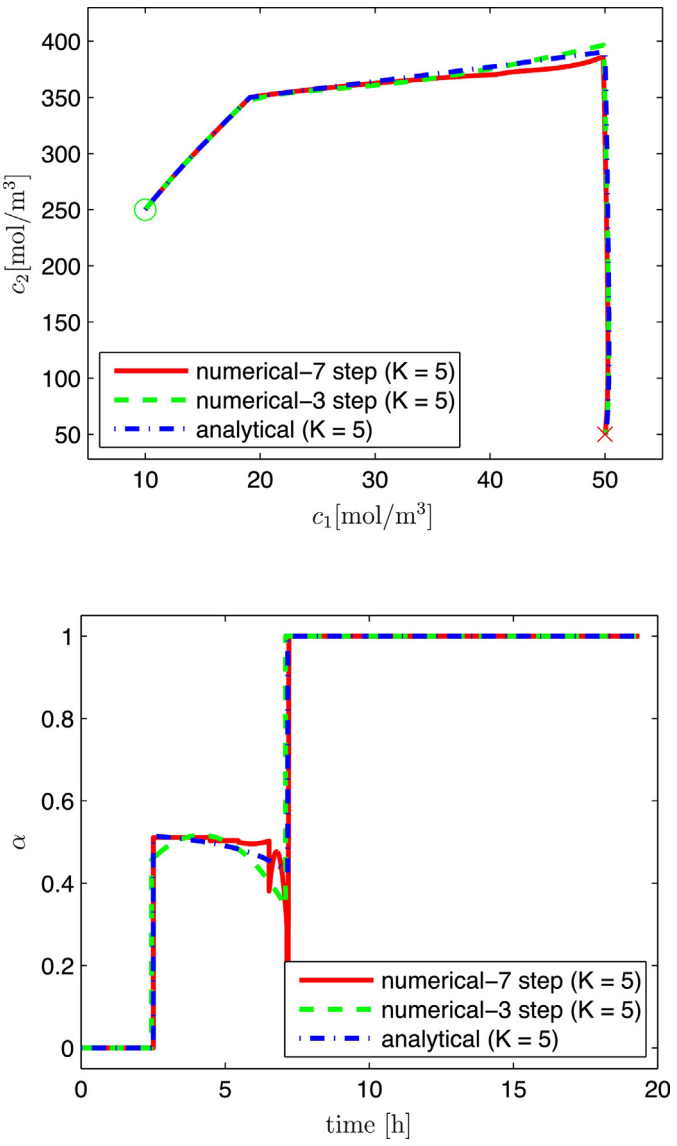

Fig. 5. Comparison of different control strategies (top – state space, bottom – control profiles).

to the fact that the rejection coefficient is close to 1 for the entire operation. Note that the analytical approach is not able to reach final concentrations perfectly due to mismatch between assumed ($R_1 = 1$) and real rejection of the macro-solute, but the differences are negligible (less than 1‰).

6. Conclusions

In this paper we studied the time-optimal control of a batch diafiltration process in the presence of fouling. The fouling behavior was described by the reduction of the permeate flux caused by the deposit of the solutes on the membrane. Using Pontryagin's minimum principle we derived candidates for optimal control. The derived optimal operation is completely analytic, and consists of three steps with singular control being the second one. The developed theory was applied on three case studies. The first two of them with different membrane models showed possible improvements over existing membrane operations. The last case study showed that the proposed optimal control strategy, obtained for the case of constant rejection coefficients, can be applied to the situation with varying solute rejections, provided the variations are not too large. Such neighboring analytical solution achieves only slight suboptimality loss compared to time-optimal operation. The obtained results indicate that by using advanced control strategy we can reduce the production costs compared to traditionally used membrane operations and avoid any numerical optimization. Thus, the proposed method can be applied to existing plants and hardware without major investments.

Acknowledgments

The authors gratefully acknowledge the contribution of the Scientific Grant Agency of the Slovak Republic under the grant 1/0053/13, the Slovak Research and Development Agency under the project APVV-0551-11 and the internal grant of the Slovak University of Technology in Bratislava for support of young researchers. The authors would like to thank for financial assistance from the STU Grant scheme for Support of Excellent Teams of Young Researchers. This contribution/publication is also the partial result of the Research & Development Operational Programme for the project University Scientific Park STU in Bratislava, ITMS 26240220084, supported by the Research 7 Development Operational Programme funded by the ERDF.

References

Aspelund, M.T., Glatz, C.E., 2010. Purification of recombinant plant-made proteins from corn extracts by ultrafiltration. J. Membr. Sci. 353, 103–110, http://dx.doi.org/10.1016/j.memsci.2010.02.036.

Baker, R.W., 2012. Membrane Technology and Applications, third ed. Wiley.

Biegler, L.T., 1984. Solution of dynamic optimization problems by successive quadratic programming and orthogonal collocation. Comput. Chem. Eng. 8, 243–248.

Bolton, G., LaCasse, D., Kuriyel, R., 2006. Combined models of membrane fouling: development and application to microfiltration and ultrafiltration of biological fluids. J. Membr. Sci. 277, 75–84, http://dx.doi.org/10.1016/j.memsci.2004.12.053.

Bryson Jr., A.E., Ho, Y.C., 1975. Applied Optimal Control, 2nd ed. Taylor & Francis Group, New York, USA.

Charfi, A., Amar, N.B., Harmand, J., 2012. Analysis of fouling mechanisms in anaerobic membrane bioreactors. Water Res. 46, 2637–2650, http://dx.doi.org/10.1016/j.watres.2012.02.021.

Čižniar, M., Fikar, M., Latifi, M.A., 2005. MATLAB Dynamic Optimisation Code DYNOPT. User's Guide. Technical Report. KIRP FCHPT STU, Bratislava, Slovak Republic.

Fikar, M., Kovács, Z., Czermak, P., 2010. Dynamic optimization of batch diafiltration processes. J. Membr. Sci. 355, 168–174, http://dx.doi.org/10.1016/j.memsci.2010.03.019.

Foley, G., 1999. Minimisation of process time in ultrafiltration and continuous diafiltration: the effect of incomplete macrosolute rejection. J. Membr. Sci. 163, 349–355.

Hermia, J., 1982. Constant pressure blocking filtration laws-application to power-law non-Newtonian fluids. Trans. Inst. Chem. Eng. 60, 183–187.

Jelemenský, M., Klaučo, M., Paulen, R., Lauwers, J., Logist, F., Van Impe, J., Fikar, M., 2016. Time-optimal control and parameter estimation of diafiltration processes in the presence of membrane fouling. In: 11th IFAC Symposium on Dynamics and Control of Process Systems, Norway (accepted for publication).

Jelemenský, M., Paulen, R., Fikar, M., Kovacs, Z., 2014. Time-optimal diafiltration in the presence of membrane fouling. In: Preprints of the 19th IFAC World Congress Cape Town (South Africa) August 24–29, 2014, pp. 4897–4902.

Jelemenský, M., Sharma, A., Paulen, R., Fikar, M., 2015. Time-optimal operation of diafiltration processes in the presence of fouling. In: Gernaey, K.V., Huusom, J.K., Gani, R. (Eds.), 12th International Symposium on Process Systems Engineering and 25th European Symposium on Computer Aided Process Engineering. Elsevier B.V., Copenhagen, Denmark, pp. 1577–1582.

Kovács, Z., Discacciati, M., Samhaber, W., 2009. Modeling of batch and semi-batch membrane filtration processes. J. Membr. Sci. 327, 164–173, http://dx.doi.org/10.1016/j.memsci.2008.11.024.

Kovács, Z., Fikar, M., Czermak, P.,2009. Mathematical modeling of diafiltration. In: Conference of Chemical Engineering. Pannonia University, Veszprem, pp. 135-135.

Li, Z., Youravong, W., H-Kittikun, A., 2006. Separation of proteases from yellowfin tuna spleen by ultrafiltration. Bioresour. Technol. 97, 2364–2370, http://dx.doi.org/10.1016/j.biortech.2005.10.019.

Luján-Facundo, M., Mendoza-Roca, J., Cuartas-Uribe, B., Álvarez-Blanco, S., 2015. Evaluation of cleaning efficiency of ultrafiltration membranes fouled by BSA using FTIR-ATR as a tool. J. Food Eng. 163, 1–8, http://dx.doi.org/10.1016/j.jfoodeng.2015.04.015.

Luo, R., Waghmare, R., Krishnan, M., Adams, C., Poon, E., Kahn, D., 2004. Process Optimization for The Ultrafiltration/Diafiltration of Abthrax Antibody to Very High Final Concentrations. Millipore Technical Publications Lit. No. PS1240EN00. Millipore Corporation, Billerica, MA 01821, USA.

Ng, P., Lundblad, J., Mitra, G., 1976. Optimization of solute separation by diafiltration. Sep. Sci. Technol. 11, 499–502.

Paulen, R., Fikar, M., Foley, G., Kovács, Z., Czermak, P., 2012. Optimal feeding strategy of diafiltration buffer in batch membrane processes. J. Membr. Sci. 411–412, 160–172, http://dx.doi.org/10.1016/j.memsci.2012.04.028.

Paulen, R., Jelemenský, M., Kovacs, Z., Fikar, M., 2015. Economically optimal batch diafiltration via analytical multi-objective optimal control. J. Process Control 28, 73–82.

Pontryagin, L.S., Boltyanskii, V.G., Gamkrelidze, R.V., Mishchenko, E.F., 1962. The Mathematical Theory of Optimal Processes. Wiley, New York, USA.

Rajagopalan, N., Cheryan, M., 1991. Process optimization in ultrafiltration: flux-time considerations in the purification of macromolecules. Chem. Eng. Commun. 106, 57–69.

Sharma, A., Jelemenský, M., Paulen, R., Fikar, M., 2016. Estimation of membrane fouling parameters for concentrating lactose using nanofiltration. In: 26th European Symposium on Computer Aided Process Engineering, Slovenia (accepted for publication).

Srinivasan, B., Palanki, S., Bonvin, D., 2003. Dynamic optimization of batch processes: I. Characterization of the nominal solution. Comput. Chem. Eng. 27, 1–26.

Takači, A., Žikić-Došenović, T., Zavargó, Z., 2009. Mathematical model of variable volume diafiltration with time dependent water adding. Eng. Comput. Int. J. Comput. Aided Eng. Softw. 26, 857–867.

Vela, M.C.V., Blanco, S.A., García, J.L., Rodríguez, E.B., 2008. Analysis of membrane pore blocking models applied to the ultrafiltration of PEG. Sep. Purif. Technol. 62, 489–498, http://dx.doi.org/10.1016/j.seppur.2008.02.028.

Yazdanshenas, M., Tabatabaeenezhad, A., Roostaazad, R., Khoshfetrat, A., 2005. Full scale analysis of apple juice ultrafiltration and optimization of diafiltration. Sep. Purif. Technol. 47, 52–57.

Zhao, Y., Wu, K., Wang, Z., Zhao, L., Li, S.S., 2000. Fouling and cleaning of membrane – a literature review. J. Environ. Sci. 12, 241–251.